

https://dspace.org/

Elastic properties of glasses and glass ceramics at high pressures and high temperatures

Gravett, Salome

2015-01-22
http://hdl.handle.net/10539/16700

Downloaded from a DSpace repository. https://dspace.org/

4. DATA ANALYSIS

As mentioned before several corrections had to be applied to the data set to obtain frequency values at true pressure and true temperature.

4.1 Pressure

For most high pressure devices, the hydraulic oil pressure is used as an indication of the sample pressure (Sigalas, et al., 1988), which can be highly inaccurate. The pressure exerted on the sample is related to the oil pressure by:

$$P_2 = P_1.A_1/A_2 \qquad (4.1)$$

where,

P_1 = oil pressure,

P_2 = sample pressure,

A_1 = ra[illegible] area,

A_2 = [illegible]ce area.

However, figure 4.1, shows a hysteresis loop obtained when a pressure-dependent parameter is plotted against pressure for both an up and down pressure stroke. This is due to friction in the system which involves friction in the seals of the hydraulic cylinder, friction between the piston and cylinder walls, interfacial friction between the cylinder and sample walls, and internal shear stresses of the various pressure transmitting media within the capsule. As the piston is pushed into the cylinder, there is a certain amount of frictional lag. Consequently the driving thrust transmitted to the piston is not completely transferred to the sample. When the thrust on the piston is released there is a backlash region in which the frictional forces reverse direction. Friction hinders the retraction of the piston from the cylinder and the capsule from expanding, and the pressure acting on the sample is higher than that calculated from equation (4.1).

To illustrate the procedure for applying friction correction, data is used

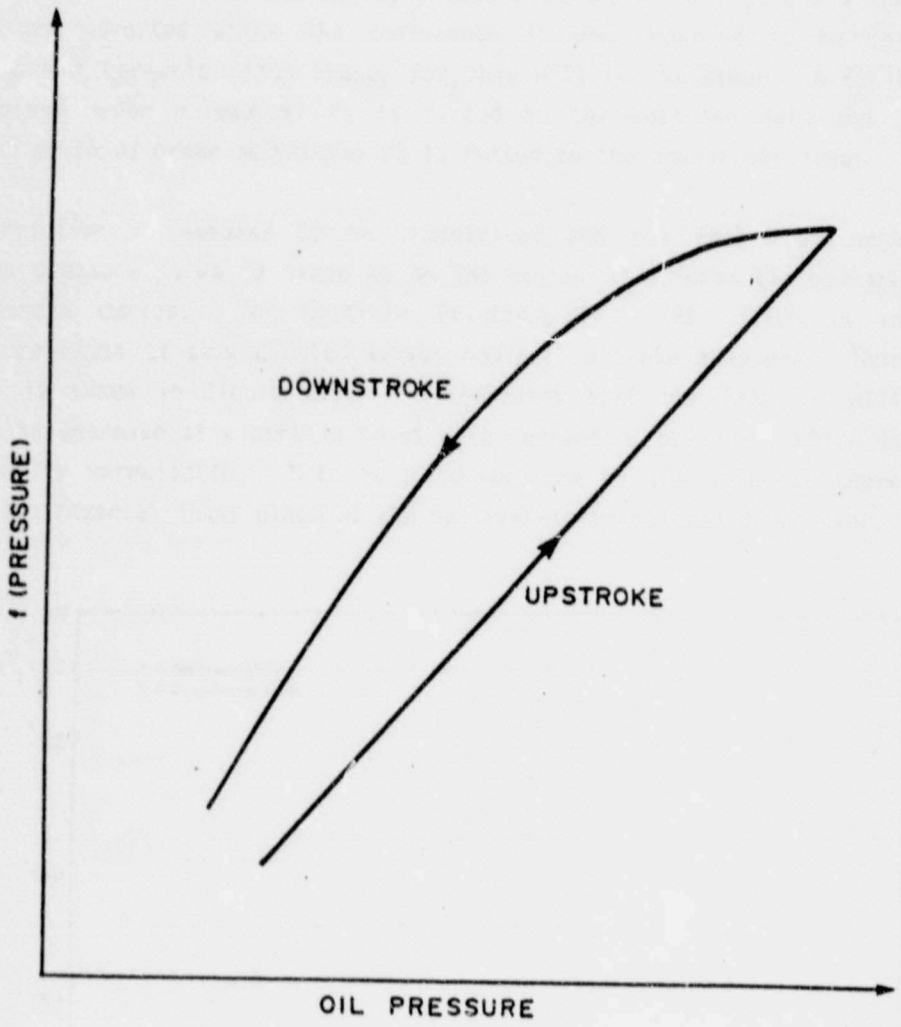

Fig. 4.1 Hysteresis loop obtained when a pressure-dependent variable f is plotted against pressure for a piston-cylinder device

which has been gathered from manganin calibration tests done using a thermal conductivity capsule of 30 mm in diameter. As shown in figure 4.2 the resistance of the manganin gauge is plotted versus pressure for both an increasing and decreasing pressure stroke. In figure 4.3 the axes are inverted where the resistance is now regarded to be the independent variable. The reason for this will become clear. A first or second order polynomial P1 is fitted to the upstroke data and a second or third order polynomial P2 is fitted to the downstroke data.

The friction is assumed to be symmetrical and the true resistance versus pressure curve is taken to be the median P3 between the up- and downstroke curves. The upstroke friction, P1 - P3, which is in pressure units is then plotted versus nominal upstroke pressure. This curve is shown in figure 4.4. It indicates that the friction will start to decrease at a certain point with increasing pressure, which is physically unrealistic. This is a consequence of the interval where friction reversal takes place at the upstroke-to-downstroke changeover.

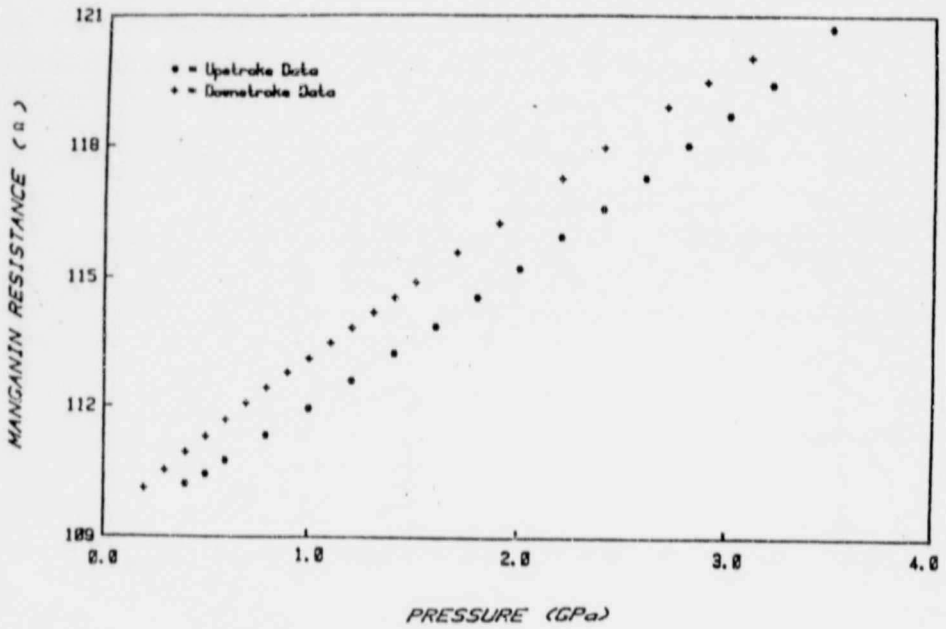

Fig. 4.2 Hysteresis curve for the resistance of a manganin gauge versus pressure

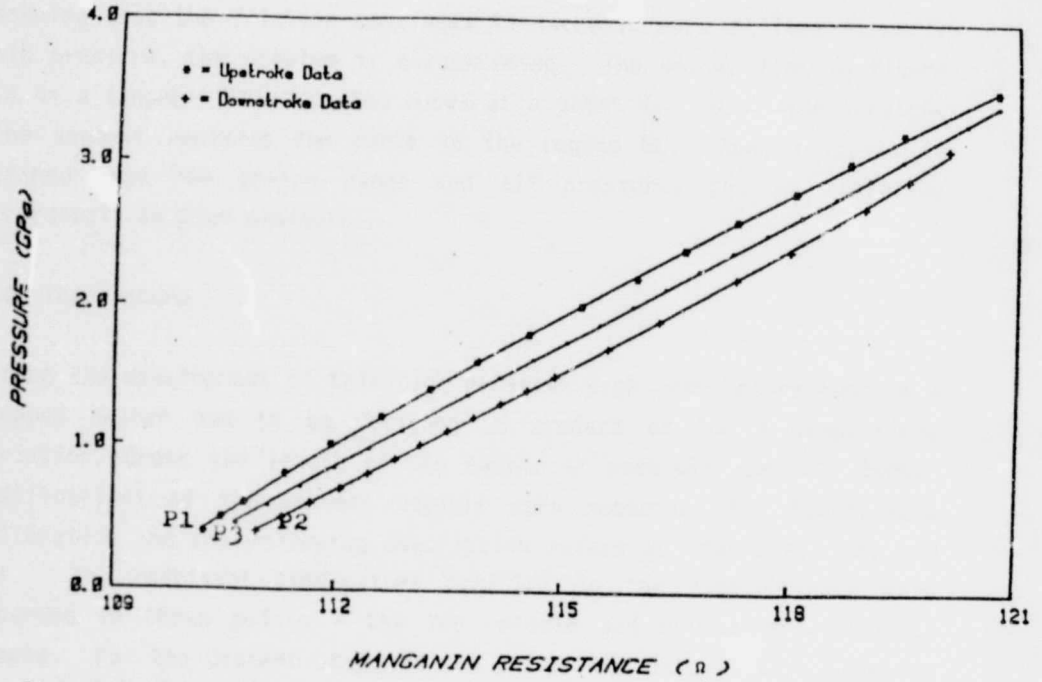

Fig. 4.3 Pressure versus resistance as the independent variable

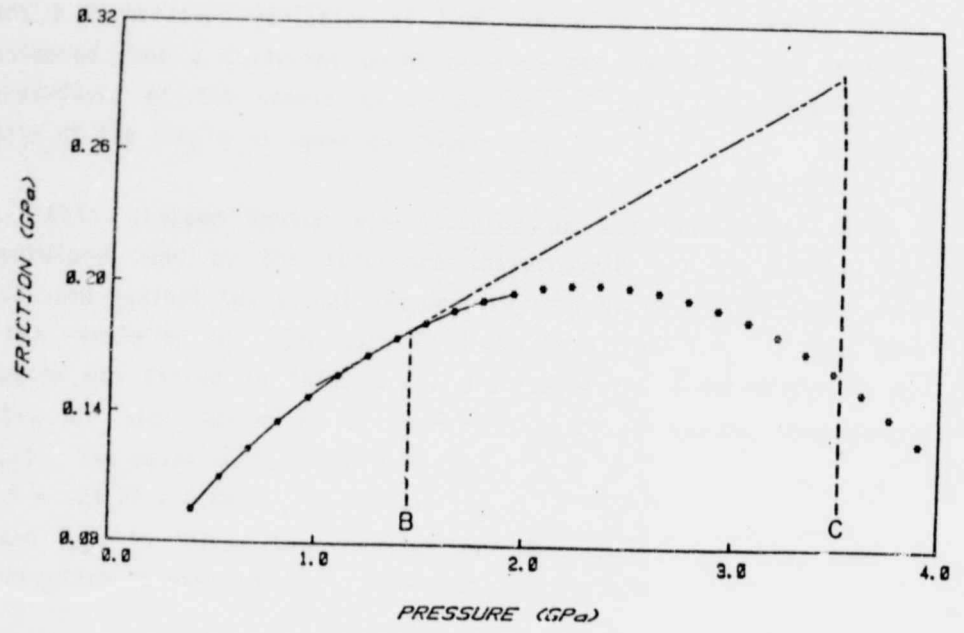

Fig. 4.4 Upstroke friction versus nominal upstroke pressure. The dotted line is a tangent fitted to the curve at B

Assuming that the friction continues to increase more or less linearly with pressure, the problem is circumvented. The dotted line in figure 4.4 is a tangent fitted to the curve at a point B. The dotted straight line segment replaces the curve in the region BC. Now, friction is defined over the entire range and all pressures can be corrected accordingly to true pressure.

4.2 Temperature

During the development of this high pressure high temperature capsule a stepped heater had to be designed to produce as low a temperature variation across the length of the sample as possible (Levitt, 1985). Modifications of the present capsule were necessary for temperature calibration and the following description refers to figure 4.5 (a) and (b). The resultant temperature profiles in the sample space were recorded in three points - the top, middle and bottom of a "dummy" sample. For the present shape of the heater the data plot is shown in figure 4.6. According to this figure, there is a variation of 27 °C along the 10 mm sample length at a mean temperature of 370 °C. This means a temperature variation of 7.3%, which is an acceptable error. Considered from a different point of view the temperature at the two end-surfaces of the sample as a function of the temperature at the middle of the sample is shown in figure 4.7.

Once this stepped heater was accepted as the most suitable, the temperature read by the reference thermocouple (figure 4.5(b)) was calibrated against the actual temperature read by the test thermocouple in the sample space. The data is shown in figure 4.8. A quadratic equation was fitted to this curve, describing the temperature in the centre of the sample as a function of the reference temperature (T_{ref}). The equation is given below:

$$T = -23.77 + 1.98\ T_{ref} + 0.00044\ T^2_{ref} \qquad (4.2)$$

(T and T_{ref} in °C). This equation was then applied in this study as a correction to experimentally recorded temperatures.

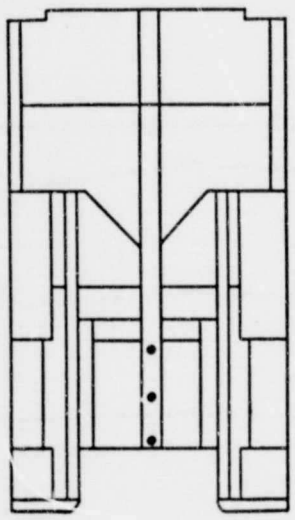

• Thermocouple beads

(a)

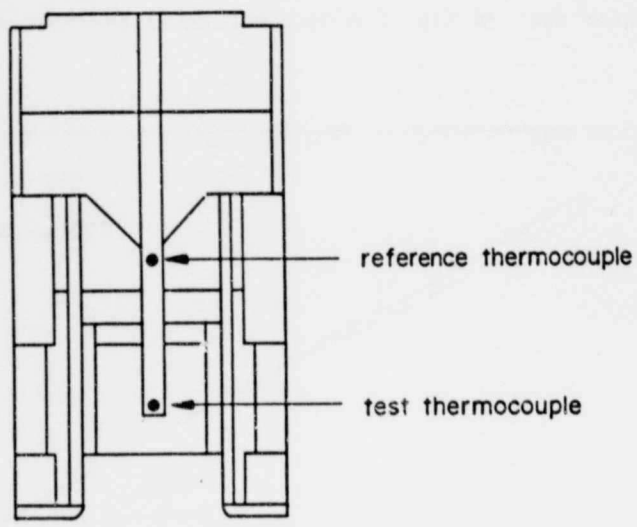

(b)

Fig. 4.5(a) Temperature profiles in the sample space had to be recorded at three points - the top, middle and bottom

(b) The temperature read by the reference thermocouple had to be calibrated against the actual temperature read by the test thermocouple in the sample space

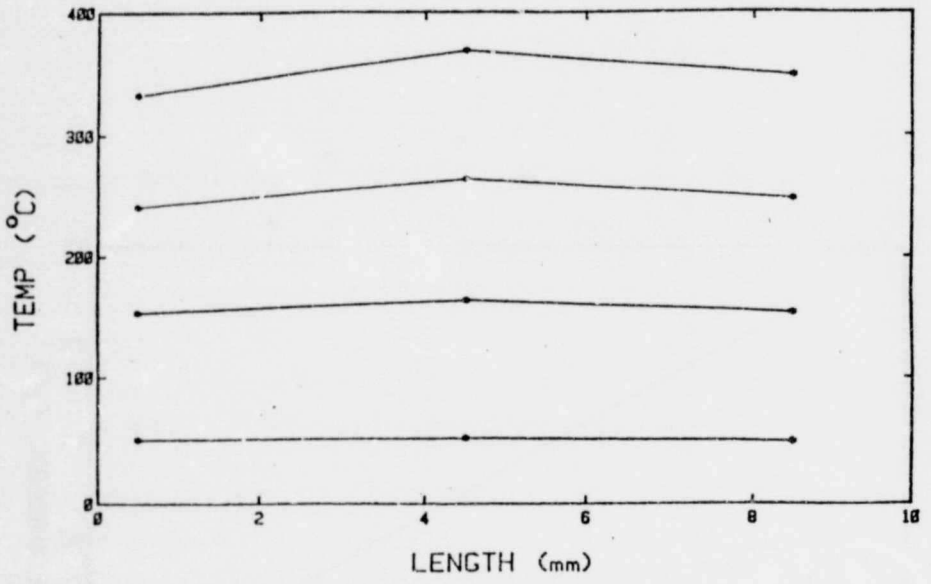

Fig. 4.6 Temperature profiles along the sample length at [illegible] temperatures

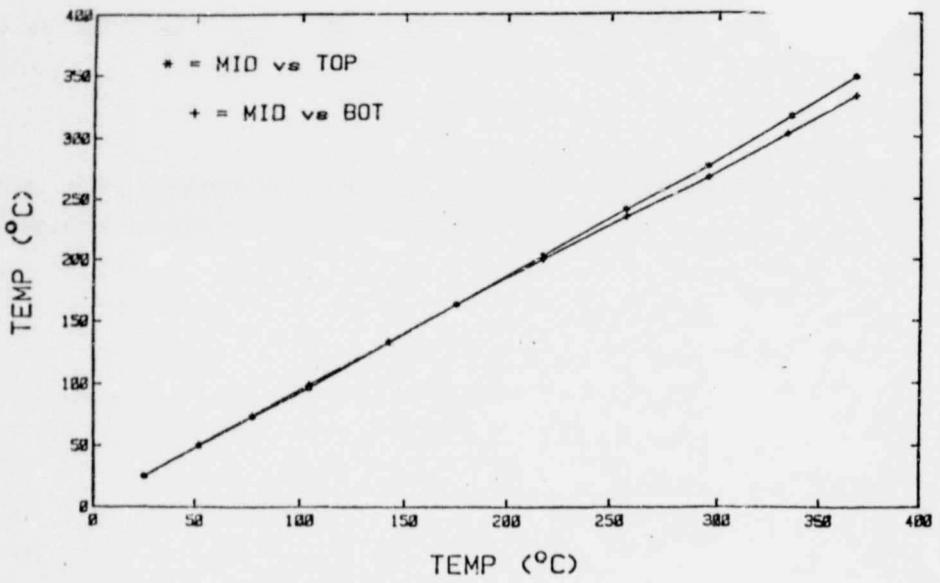

Fig. 4.7 Temperature at two end surfaces of sample (top and bottom) as a function of temperature at the middle of the sample

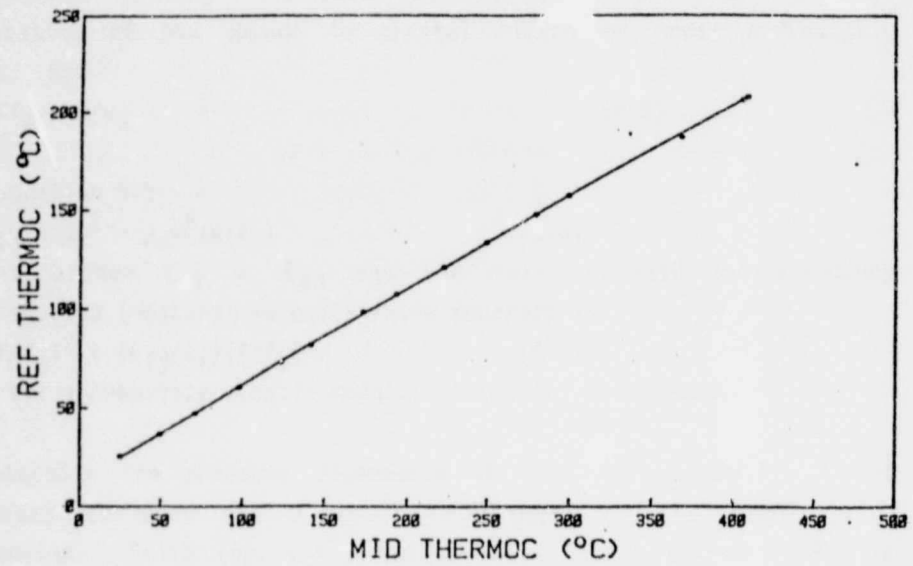

Fig. 4.8 Temperature read by the reference thermocouple versus temperature read by the test thermocouple

4.3 Elastic moduli

From equation (3.2) it is clear that

$$v = 2\ell f \tag{4.3}$$

while f is related to the natural velocity, w, by

$$w = 2\ell_0 f \tag{4.4}$$

Zero subscript implies the value at atmospheric pressure. The concept of "natural velocity" has been used to bypass the requirement of calculation of the change in crystal dimensions under hydrostatic stress. Now

$$f/f_0 = w/w_0 \tag{4.5}$$

From equation 3.1

$$C_{ij} = \rho v^2 = \rho_0 w^2 (\ell/\ell_0) \tag{4.6}$$

C_{ij} is either C_{11} or C_{44} and the relation with the frequency ratio squared (=natural velocity ratio squared) is

$$(f/f_0)^2 = (C_{ij}/C_0)(\ell/\ell_0) \tag{4.7}$$

C_0 is the appropriate elastic modulus at ambient conditions.

To determine the pressure dependence of the elastic moduli, it is necessary to know the dimensional changes of the sample with compression. Fritz (op. cit.) has modified Cook's method (1957) to account for the anomalous behaviour demonstrated by a lithia-alumina-silica glass ceramic at high pressure. This anomalous behaviour could possibly be related to a structural phase transformation, spread out over a range of pressures. In the case of a first-order pressure-induced transition, Cook's method is not valid in the vicinity of the transition because of a discontinuous volume change. For a smeared out transition, it is not known a priori whether Cook's method is valid. In this case, the static compressibility could conceivably be greater than that determined from ultrasonic data, and the usual self-consistent calculation of elastic constants and volume compression would give erroneous results. With Fritz's method it is assumed as a first approximation that the compressibility of the material is constant as a function of pressure.

This compressibility is calculated from C_{11} and C_{44} at ambient temperature and pressure. The sample compression as a function of pressure is then calculated by numerical integration using small pressure intervals. This first approximation of the compression is then combined with values from smooth curves through (f/f_0) versus pressure data to calculate the first approximation of the elastic constants as a function of pressure. This is done by using the equation

$$C_{ij} = C_0(\ell_0/\ell)(f/f_0)^2 \qquad (4.8)$$

The second step is the same as the first one, except that the compressibility is not being assumed constant but calculated from the pressure-dependent elastic constants from the first step. By numerical integration, a second approximation to the compression curve is generated and this is once again combined with the (f/f_0) versus pressure data to determine the second approximation for the elastic constants as a function of pressure, again using equation (4.8). The above described calculation may be iterated as many times as needed for convergence. For this study the calculation was iterated five times.

It is now possible, using the corrections discussed in this chapter to calculate the pressure dependence at various temperatures of the bulk modulus, the Young's modulus, the Lamé constant and the Poisson's ratio. The volumetric compression is deduced from the bulk modulus and its hydrostatic pressure derivative, using the Murnaghan (1944) equation of state

$$\ln(V/V_0) = -1/B' \ln[B_0'(P/B_0)+1] \qquad (4.9).$$

which assumes that the bulk modulus depends linearly on pressure:

$$B(P) = -V(\partial P/\partial V)_T = B_0 + P(\partial B/\partial P)_{P=0,T}$$
$$= B_0 + PB_0'$$

5. RESULTS AND DISCUSSION

5.1 Zerodur glass ceramic

Zerodur (a product of Jenaer Glasswerk, Schott und Gen.) is a glass ceramic having practically zero thermal expansion at room temperature (Gerlich and Wolf, op. cit.). The chemical composition varies slightly from one batch to another, but a typical example is shown in table 5.1.1.

Table 5.1.1
Typical Composition of Zerodur in WT%

SiO_2	Al_2O_3	P_2O_5	Li_2O	ZnO	MgO	TiO_2	ZrO_2	Na_2O	As_2O_3
55,5	25,3	7,9	3,7	1,4	1,0	2,3	1,9	0,5	0,5

Glass ceramics with compositions based on the lithia-alumina-silica system (LiO_2-Al_2O_3-SiO_2), particularly $LiAlSi_2O_6$ III, can be made to have an extremely small thermal expansion coefficient explaining this property of Zerodur. This behaviour may be explained in terms of the repulsion existing between Si,Al and Li atoms in $LiAlSi_2O_6$ (Li, 1968). Each Li tetrahedron shares two edges with two Si,Al tetrahedra. All the four atoms involved in each edge sharing, i.e., Si,Al, the neighbouring Li, and two edge sharing oxygen atoms, were found to be exactly coplanar. The very short distance between Si,Al and Li, i.e., 2.609 Å, indicates the presence of a strong repulsive force between them. Upon heating, thermal energy is used to reduce the strong repulsive force by increasing the Si,Al-Li distance which, in turn, decreases the shared edge, and likely the Li-O distance. The Li-O distance would be longer when Si,Al-Li becomes shorter and vice versa. In this structure, a, and b axes are functions of the Si,Al-Li distance alone, i.e.,
a = b = 2(Si,Al-Li), and the c axes is a function of shared edge and the Li-O distance as is illustrated in figure 5.1.1. Hence upon heating, the a and b axes may be expected to expand and the c axis may be expected to contract. As a result of this kind of anisotropic thermal expansion, the overall volume may remain almost unchanged. It is very likely that the

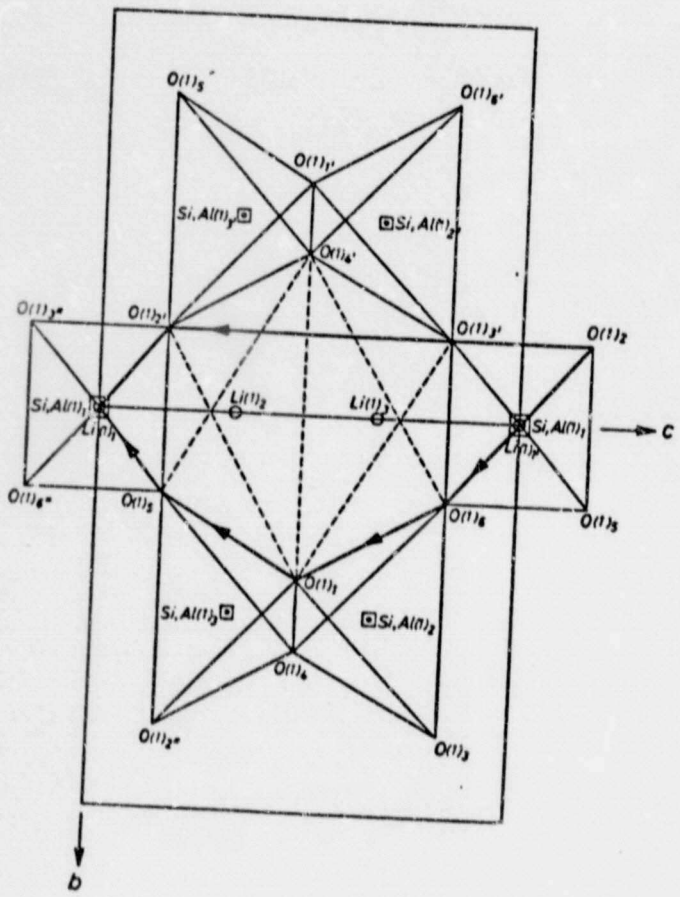

Fig. 5.1.1 Thermal expansion behaviour of c axis (after Li, 1968)

bond lengths and angles within each Si,Al tetrahedron may change very little and the only significant changes may occur in the angles between the neighbouring tetrahedra.

These glass ceramics with practically zero thermal expansion are materials with a variety of interesting properties which appear to be related to the fact that they have an open crystallographic structure (Fritz, op. cit.). Therefore it is expected that high pressure would produce interesting responses in these materials. If enough pressure could be applied it may be possible to transform them to a denser crystallographic structure.

The behaviour of the elastic properties of Zerodur was investigated in this study as a function of pressure at 18 °C, 72 °C, 103 °C and 152 °C. Figures 5.1.2 and 5.1.3 show the results for the experimentally measured longitudinal and shear frequencies. These data show that both the longitudinal and shear mode frequencies decrease nonlinearly with pressure to -1.5 GPa, whereafter the longitudinal mode starts to increase with increasing pressure and the shear mode decreases more slowly. These interesting responses signify a phase transformation. This matter will be discussed later on.

The longitudinal and shear moduli were calculated using the above data and are plotted versus pressure in figures 5.1.4 and 5.1.5. It is evident that Zerodur shows the same anomalies as fused silica and other silica-rich glasses, i.e. negative pressure derivatives and an increase in the longitudinal and shear modes with temperature increase. It is interesting to note that the turning points are an increasing function of temperature.

In order to determine the pressure dependence of the elastic moduli, the dimensional changes of the sample under pressure have been applied to the above data (section 4.3). The results are displayed in figure 5.1.6 and 5.1.7 where C_{11} and C_{44} versus pressure appear. The other elastic properties, Young's modulus, the Lamé constant, Poisson's ratio and the bulk modulus were then calculated and plotted against pressure in figures 5.1.8-11. It is difficult to represent the changes in the properties over the whole range of applied pressure in terms of a simple polynomial function. Therefore for each curve the range was divided into a

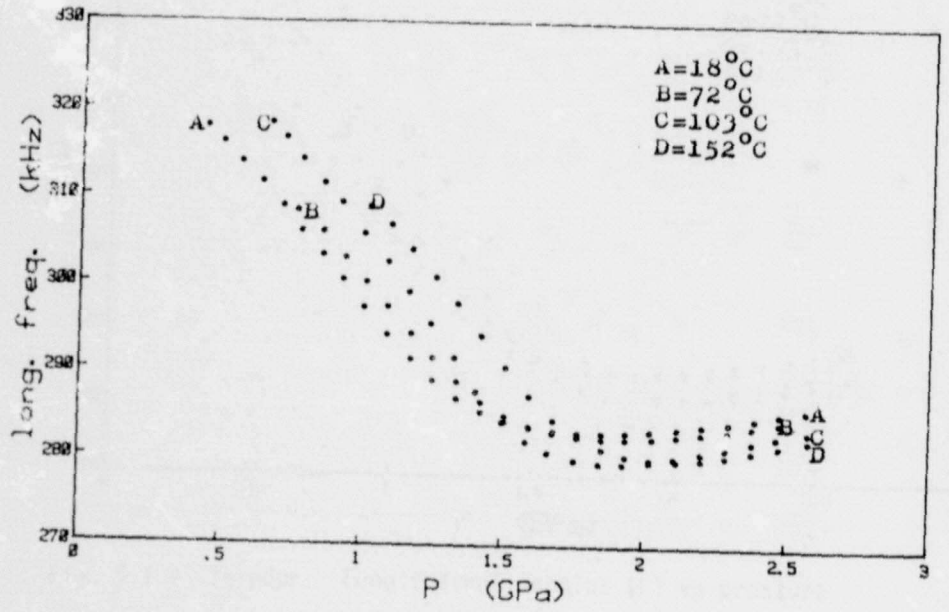

Fig. 5.1.2 Zerodur: Longitudinal frequency (long. freq.) vs pressure (P) for four isotherms

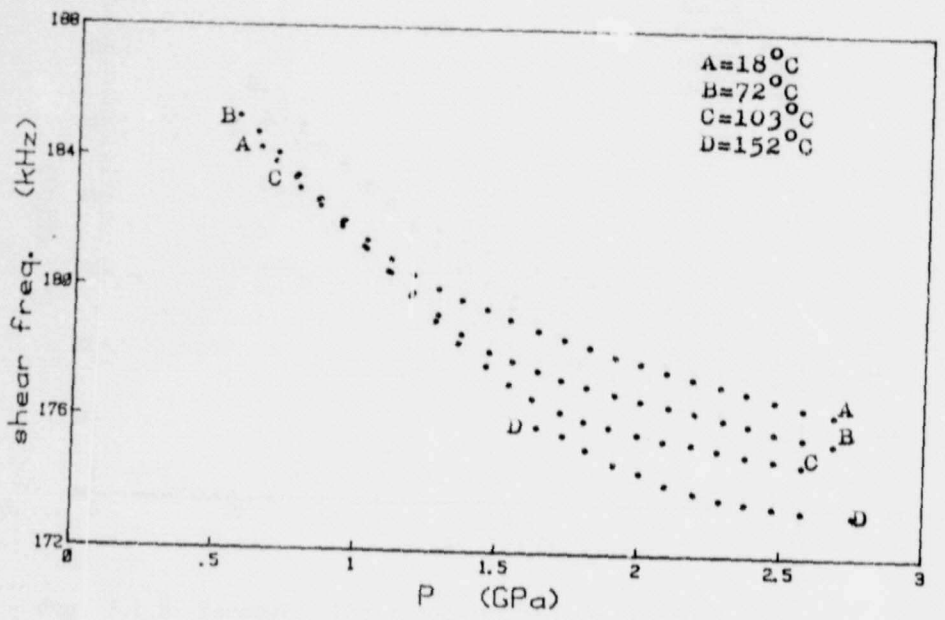

Fig. 5.1.3 Zerodur: Shear frequency (shear freq.) vs pressure for four isotherms

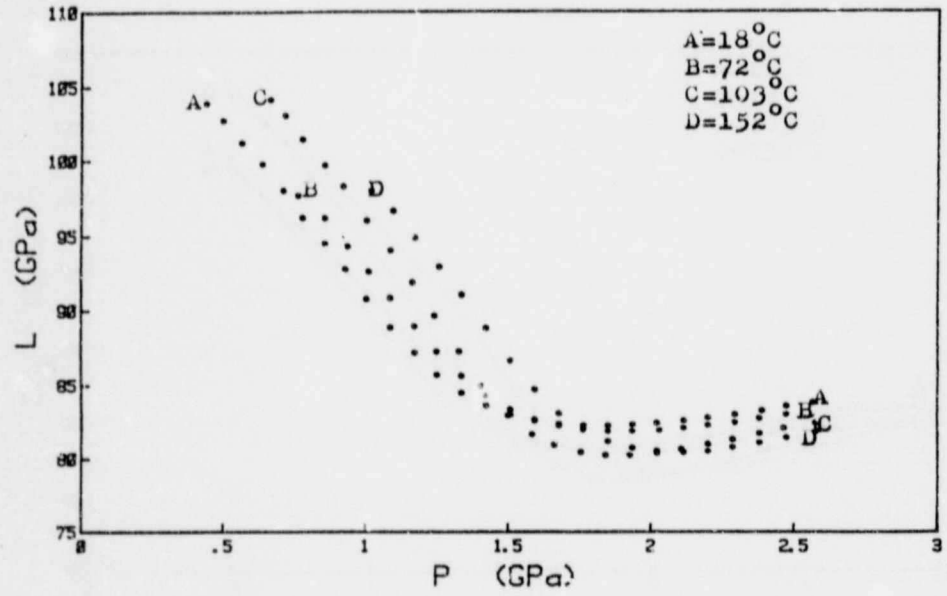

Fig. 5.1.4 Zerodur: Longitudinal modulus (L) vs pressure

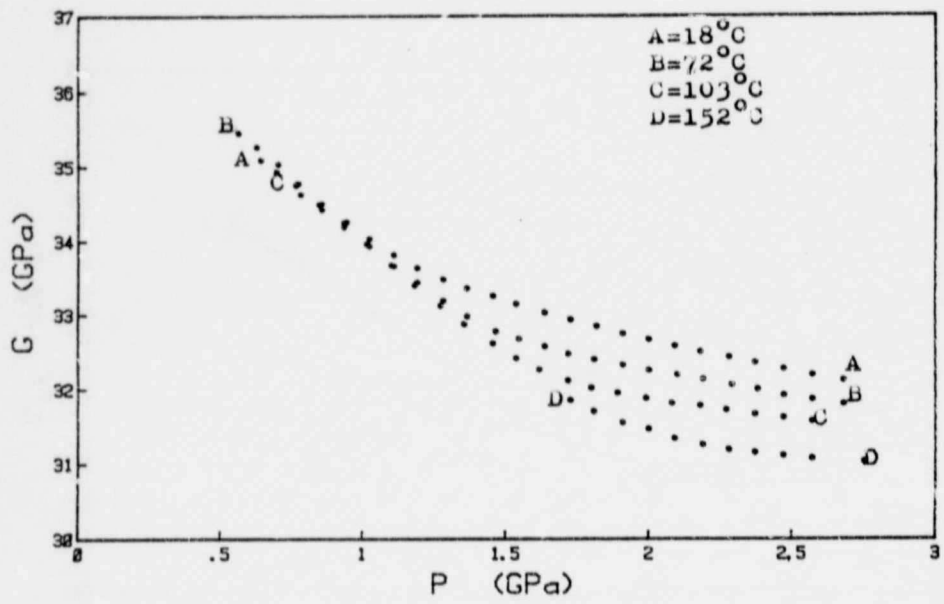

Fig. 5.1.5 Zerodur: Shear modulus (G) vs pressure

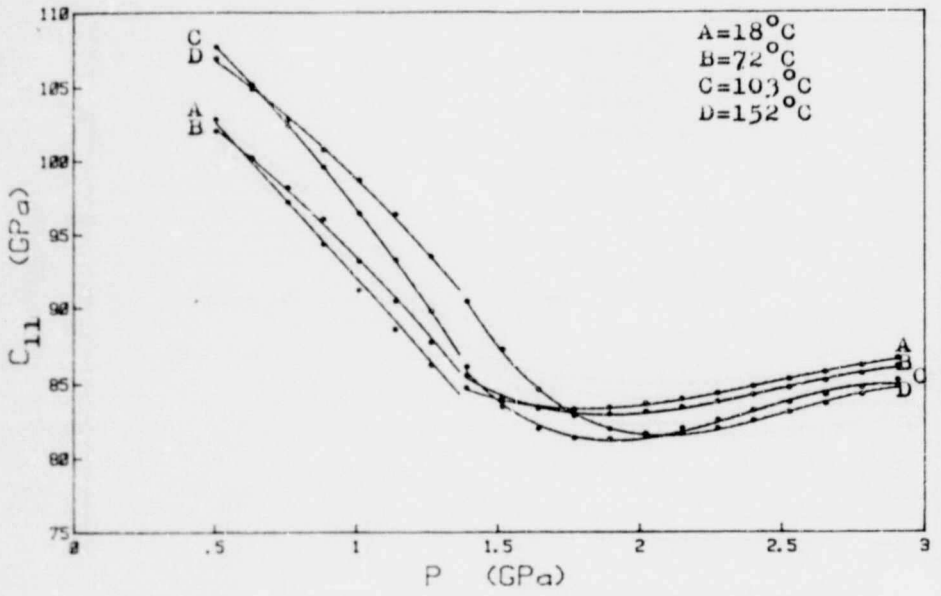

Fig. 5.1.6 Zerodur: C_{11} vs pressure

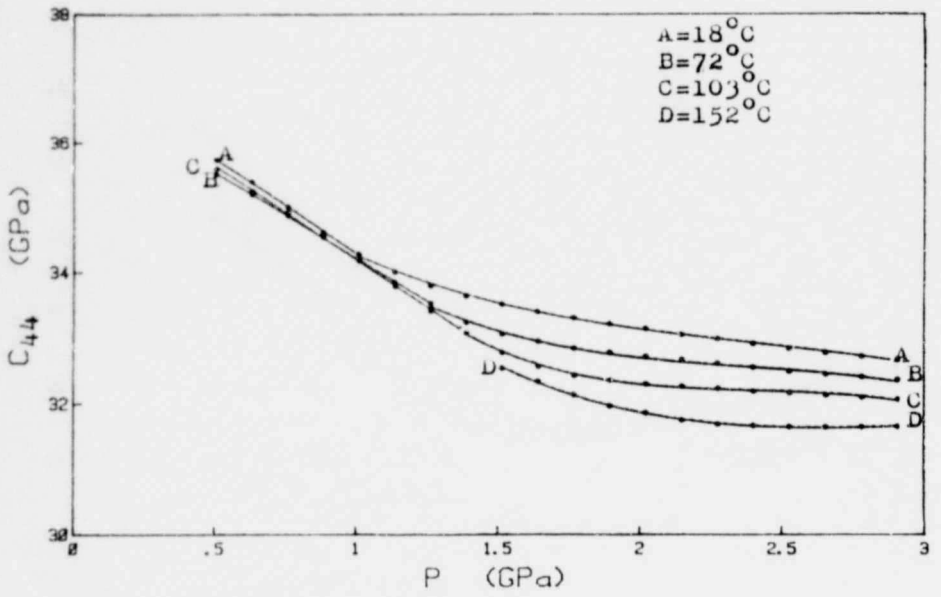

Fig. 5.1.7 Zerodur: C_{44} vs pressure

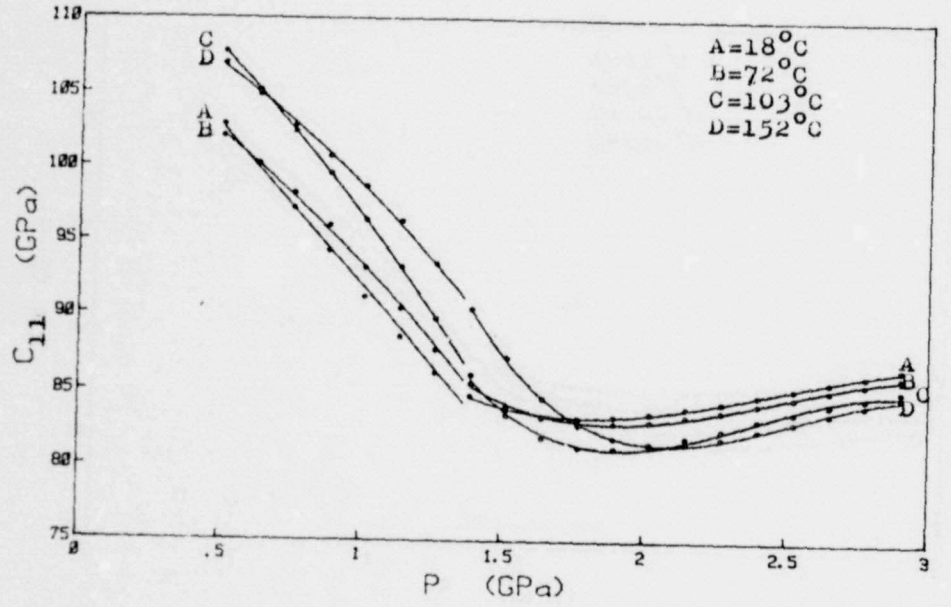

Fig. 5.1.6 Zerodur: C_{11} vs pressure

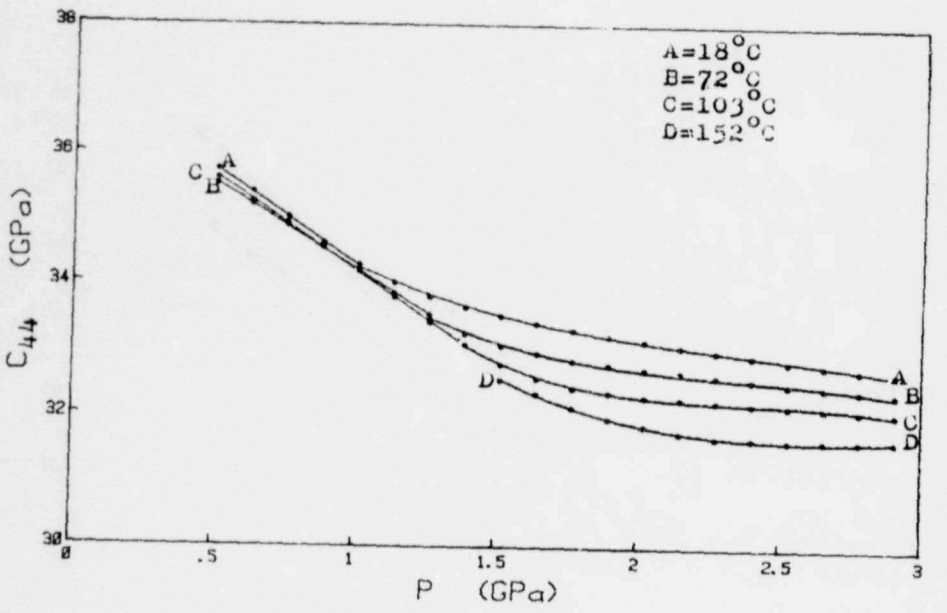

Fig. 5.1.7 Zerodur: C_{44} vs pressure

Author Gravett Salome
Name of thesis Elastic Properties Of Glasses And Glass Ceramics At High Pressures And High Temperatures. 1989

PUBLISHER:
University of the Witwatersrand, Johannesburg
©2013

LEGAL NOTICES:

Copyright Notice: All materials on the University of the Witwatersrand, Johannesburg Library website are protected by South African copyright law and may not be distributed, transmitted, displayed, or otherwise published in any format, without the prior written permission of the copyright owner.

Disclaimer and Terms of Use: Provided that you maintain all copyright and other notices contained therein, you may download material (one machine readable copy and one print copy per page) for your personal and/or educational non-commercial use only.

The University of the Witwatersrand, Johannesburg, is not responsible for any errors or omissions and excludes any and all liability for any errors in or omissions from the information on the Library website.